Inorganic Chemistry

Article

pubs.acs.org/IC

Enhanced Luminescence in Ln^{3+}-Doped Y_2WO_6 (Sm, Eu, Dy) 3D Microstructures through Gd^{3+} Codoping

Anna M. Kaczmarek,*[,†] Kristof Van Hecke,[‡] and Rik Van Deun*[,†]

[†]L^3 – Luminescent Lanthanide Lab, Department of Inorganic and Physical Chemistry, Ghent University, Krijgslaan 281-S3, B-9000 Ghent, Belgium

[‡]XStruct, Department of Inorganic and Physical Chemistry Ghent University, Krijgslaan 281-S3, B-9000 Ghent, Belgium

Supporting Information

ABSTRACT: Microstructures of Y_2WO_6 were prepared by applying a hydrothermal synthesis in the presence of sodium dodecyl sulfate (SDS) surfactant, after which the materials were heat-treated at a temperature of 1100 °C. When prepared at pH 3, the spherical 3D microstructures were built from nanosized particles. Raising the pH gave materials built from differently shaped building blocks, which influenced the final architecture. These materials, similarly to other previously investigated and reported rare-earth tungstate materials, were found to show very interesting luminescence properties. However, quantum yield (QY) values have scarcely been reported for such materials. In this work, a detailed study of the photoluminescence characteristics, decay times, and quantum yields of Y_2WO_6 doped with Sm^{3+}, Eu^{3+}, and Dy^{3+} is presented. When doped with different concentrations of Ln^{3+} ions, the luminescence properties of the samples changed. The 2.5% Dy:Y_2WO_6 sample gave white-light emission and showed a QY of 17%. For the optimal lanthanide-ion concentrations, the systems were codoped with 2% and 10% Gd^{3+} ions to test the possible enhancement of luminescence through energy transfer from W−O and/or Gd^{3+} to Ln^{3+}. The Eu^{3+},Gd^{3+}-codoped system showed QYs as high as 79%. The Sm,Gd-codoped system showed the highest enhancement of QY. After incorporation of Gd^{3+} ions, the 2.5% Sm_10% Gd:Y_2WO_6 materials showed a QY approximately 2.4 times larger than that of the 2.5% Sm:Y_2WO_6 material.

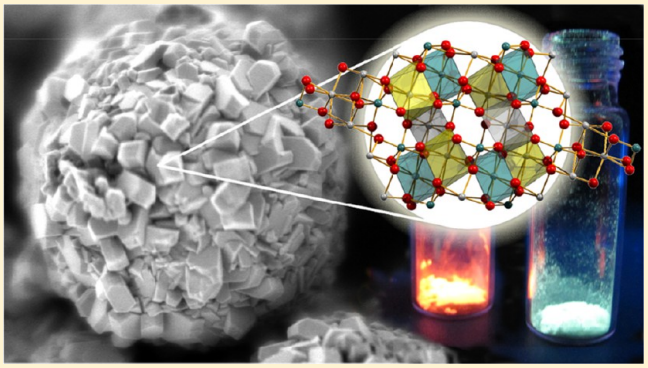

1. INTRODUCTION

Inorganic compounds doped with trivalent lanthanide ions are widely used as luminescent materials in lighting and displays,[1] lasers,[2] and scintillators.[3] The luminescence of these ions is a result of transitions within the partially filled 4f shell. These transitions are parity-forbidden, leading to low molar absorption coefficients and long luminescent lifetimes.[4]

Rare-earth tungstate and molybdate nano- and microsized materials have received quite a considerable amount of attention in the past few years. When doped with trivalent lanthanide ions, these materials have proven to have interesting luminescence properties with potential applications in various fields. One of the most promising aspects of these materials is white-light generation from a single material. As the rare-earth tungstate/molybdate matrix itself emits a blue-green color, in combination with the characteristic narrow-line emission of doped lanthanide ions, it can yield white light.[5] Many reports have been published on the syntheses and morphologies of rare-earth tungstate and molybdate materials, as well as the luminescence properties of these materials when doped with different lanthanide ions. Rare-earth (RE) tungstate materials such as RE_2WO_6, $RE_2(WO_4)_3$, and $NaRE(WO_4)_2$ have been obtained using a variety of synthetic techniques such as the hydrothermal method (which is the most often employed synthetic technique for these materials), microwave-assisted hydrothermal method, molten salt synthesis, sol−gel synthesis, and others. Factors such as the presence of a ligand, reaction time and temperature, reaction pH, and source of rare-earth and tungstate ions were found to be most important in attempts to obtain a material with specific morphology. This research was thoroughly outlined by two of us in a recent review on rare-earth tungstate and molybdate materials.[6] In the past few months, several new publications on rare-earth tungstate and molybdate particles have been published.[7−10] For example, $NaLa(WO_4)_2$ microspindles synthesized hydrothermally in the presence of disodium ethylenediaminetetraacetate (Na_2EDTA) were reported by Liu et al.[7] The morphology of this material could be easily tuned by changing certain reaction parameters, such as the amount of ligand and the ratio of water and ethanol used in the reaction. Codoping this material with Eu^{3+}/Tb^{3+}/Tm^{3+} gave a novel single-phase white-light-emitting phosphor. Zhou et al. reported the formation of $AgRE(WO_4)_2$ (RE = Y^{3+}, La^{3+}, Gd^{3+}, Lu^{3+})

Received: March 13, 2014
Published: August 28, 2014

dx.doi.org/10.1021/ic5005837 | Inorg. Chem. 2014, 53, 9498−9508

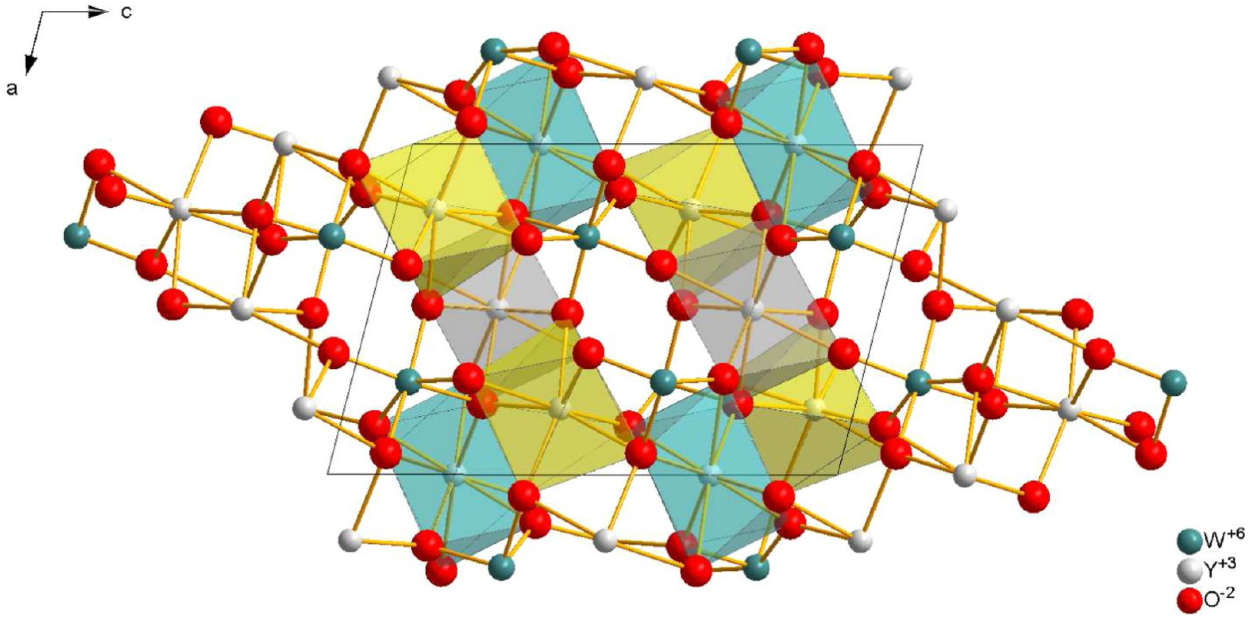

Figure 1. Crystal structure of monoclinic Y_2WO_6 in the $P2/c$ space group. Different-colored polyhedra represent nonequivalent Y^{3+} sites.

microstructures in a hydrothermal process in the presence of poly(vinylpyrrolidone) (PVP).[8] It was observed that the pH of the solution played a significant role in the formation of the final product. After codoping of these materials with various lanthanide ions, excellent up- and downconversion luminescence was reported. Some of these materials showed white-light emission.

In this research, sodium dodecyl sulfate (SDS) surfactant was used as a ligand to control the size and shape of the material. This ligand is known to form complexes with metal ions and, therefore, to slow the nucleation and growth of the crystals. Additionally, as the functional groups of the ligand bind to the surface of the material, this affects the growth rate of certain crystal facets.[11,12] To the best of our knowledge, there has been no systematic study of the effect of SDS on the morphology of rare-earth tungstate materials. The influence of pH on the phase and morphology of Y_2WO_6 were tested. Materials synthesized at pH 3 were found to give a pure phase and were used in the remainder of this research.

Despite all of the research on lanthanide-doped rare-earth tungstates, there is still a lack of detailed luminescence data beyond recorded emission and excitation spectra and calculated CIE (Commission Internationale de l'Eclairage, or International Commission on Illumination) coordinates. Therefore, we performed a detailed luminescence study of a new 3D microstructured Y_2WO_6 material doped with Sm^{3+}, Eu^{3+}, and Dy^{3+} (doped with different ion concentrations of 2.5%, 5%, and 10%) and its precursor material. The absolute quantum yields of Ln^{3+}-doped Y_2WO_6 microstructures were determined and showed rather high values for some of the materials. For the determination of absolute quantum yields, a calibrated stand-alone integrating sphere was employed. To the best of our knowledge, absolute quantum yield values of lanthanide-doped rare-earth tungstate microsized materials were only recently reported.[13] The quantum yields of Eu^{3+}-doped $RE_2(WO_4)_2$ (RE = Y^{3+}, La^{3+}, Gd^{3+}, Lu^{3+}) were reported to be very high, especially for Eu^{3+}-doped $Lu_2(WO_4)_2$ (95%) and Eu^{3+}-doped $Y_2(WO_4)_2$ (90%). Also, very recently, Zhou et al. reported quantum yield values for double rare-earth silver tungstate materials $AgRE(WO_4)_2$ (RE = Y^{3+}, La^{3+}, Gd^{3+}, Lu^{3+}) that were also very promising.[8]

This study was undertaken with two motivations: First, it was intended to investigate the absolute quantum yield values of a different lanthanide-doped tungstate material for which these values have not yet been reported in the literature. Y_2WO_6 materials doped with different concentrations of lanthanides that emit light in the visible region were studied. The detailed luminescence properties of these microstructures are presented in this article. The second motivation was to try to enhance the luminescence of these materials by codoping Gd^{3+} ions into the matrix. To the best of our knowledge, this approach has not been applied before for any of the rare-earth tungstate materials.

2. EXPERIMENTAL SECTION

All chemicals (analytical-grade) were purchased from Sigma-Aldrich and used without further purification.

2.1. Synthesis of Ln-Doped Y_2WO_6 (Ln = Sm^{3+}, Eu^{3+}, Gd^{3+}, Dy^{3+}). Samples were synthesized hydrothermally in the presence of SDS. First, 1 mmol of SDS was dissolved in 20 mL of distilled water. Separately, 1 mmol of $RE(NO_3)_3$ salt at the right percentage was weighed and dissolved in 10 mL of water. The salt solution was slowly added to the SDS solution under stirring on a magnetic stirrer. After 15 min, 1 mmol of Na_2WO_4 dissolved in of 10 mL water was slowly added, and the pH value of the solution was adjusted to 3, 7, or 10 by addition of dilute HNO_3 or NaOH. The total volume of the solution was adjusted to 50 mL by adding the right amount of water. After 10 min, the mixture was transferred into an autoclave, which was sealed and heated at 200 °C for 24 h (at an oven heating rate of 1 °C/min). The autoclave was allowed to cool naturally to room temperature, the precipitate was separated by centrifugation, and the product was washed twice with water and twice with ethanol and then dried at 60 °C in a vacuum oven. The as-prepared samples are referred to as the "precursors" throughout this article. Next, the synthesized products were heat-treated in air at 1100 °C for 3 h.

2.2. Characterization. Scanning electron microscopy (SEM) measurements were performed with an FEI Quanta 200 F scanning electron microscope and an FEI Nova 600 Nanolab dual-beam focused-ion-beam instrument in secondary electron mode. X-ray diffraction (XRD) patterns were recorded on a Thermo Scientific ARL X'TRA diffractometer equipped with a Cu K_α (λ = 1.5405 Å) source, a

dx.doi.org/10.1021/ic5005837 | Inorg. Chem. 2014, 53, 9498−9508

goniometer, and a Peltier-cooled Si(Li) solid-state detector. The luminescence properties of solid samples were studied. Solid powdered samples were placed between quartz plates (Starna cuvettes for powdered samples, type 20/C/Q/0.2). Photoluminescence measurements were performed on an Edinburgh Instruments FLSP920 UV–vis–NIR spectrofluorimeter, using a 450-W xenon lamp as the steady-state excitation source and a Hamamatsu R928P photomultiplier-tube (PMT) detector, with a response curve between 200 and 900 nm. Luminescence decay times were recorded using a 60-W pulsed Xe lamp, operating at a frequency of 100 Hz. Absolute quantum yields (QYs) were measured in an integrating sphere, coated on the inside with BENFLEC, provided by Edinburgh Instruments. The error in QY measurements was estimated to be around 10%. All of the luminescence measurements were recorded at room temperature. To compare the measurements, the same amounts of powder were used, along with the same settings for each measurement (same step, slit size, and dwell time). All emission spectra included in this article have been corrected for detector sensitivity. The excitation spectra, however, have not been corrected for detector sensitivity (see Figure S1 of the Supporting Information for an explanation). The CIE color coordinates, as well as color temperatures, were calculated using the ColorCalculater 4.97 freeware program provided by Osram Sylvania.

3. RESULTS AND DISCUSSION

3.1. Structure and Morphology. Yttrium oxytungstate, Y_2WO_6 or $Y_2O_3{\cdot}WO_3$, was first reported by Borchardt in 1963.[14] Crystal structures of Y_2WO_6 in three different space groups, namely, $P2/c$, $P2_12_12_1$, and $P4/nmm$ (where Y_2WO_6 in the $P2_12_12_1$ space group has two polymorphs with different unit cells), have been reported in the literature and can be found in the Inorganic Crystal Structure Database (ICSD).[15−18] The XRD patterns of two samples annealed at 1100 °C were matched with the XRD pattern of monoclinic Y_2WO_6 calculated using the Mercury crystal structure visualization, exploration, and analysis tool (Figure S2, Supporting Information). Monoclinic Y_2WO_6 is in the $P2/c$ space group with a = 7.589 Å, b = 5.334 Å, c = 11.354 Å, β = 104.41°, and Z = 4. The XRD patterns of the two annealed samples were also consistent with the standard monoclinic Y_2WO_6 Joint Committee on Powder Diffraction Standards pattern (JCPDS no. 73-0118). The crystal structure of monoclinic Y_2WO_6 is shown in Figure 1. As can be seen from the structure, there are three nonequivalent Y^{3+} lattice sites. Two of these lattice sites are eight-coordinated by eight O^{2-} ions, and one Y^{3+} lattice site is coordinated by seven O^{2-} ions. Each of the W^{6+} ions is surrounded by six oxygen ions and form WO_6 octahedra. The ionic radii of the Ln^{3+} ions (Ln = Eu^{3+}, Sm^{3+}, Gd^{3+}, Dy^{3+}) resemble the Y^{3+} ionic radius more than the W^{6+} ionic radius. Therefore, the doped lanthanide ions occupy the Y^{3+} crystallographic sites. The Ln^{3+} ions can substitute the Y^{3+} ions in any of the three crystallographic sites with equal probability.

The XRD patterns of the precursor samples could not be matched with any standard XRD patterns found in the JCPDS database. Other reported rare-earth tungstate precursor materials synthesized in the presence of surfactants also could not be matched with known XRD patterns.[19,20] Figure 2 shows XRD patterns of the yttrium oxytungstate samples prepared at pH 3, 7, and 10 after annealing at 1100 °C. This annealing temperature was chosen based on the observations made by Wang et al.[21] In their study, they showed that lower annealing temperatures (650 or 750 °C) gave metastable forms of Y_2WO_6. As can be seen in Figure 2, when the reaction was carried out at pH 3, a pure monoclinic Y_2WO_6 phase with no additional peaks formed. When the starting reaction solution

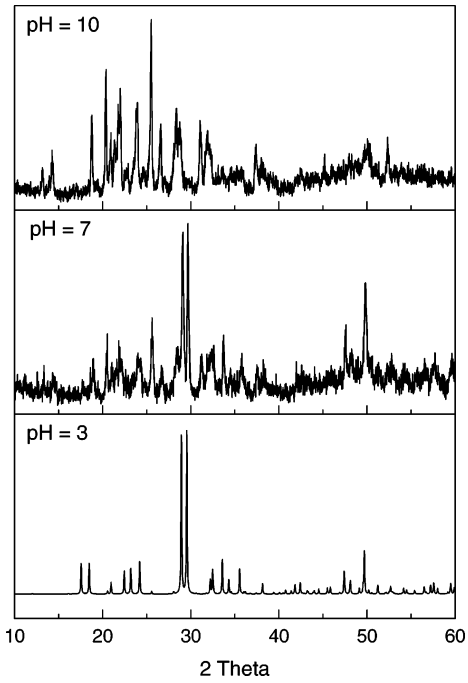

Figure 2. XRD patterns of materials obtained at different pH values (pH 3, 7, and 10) and annealed at 1100 °C for 3 h.

was adjusted to neutral pH, the characteristic XRD patterns of a monoclinic Y_2WO_6 phase can be distinguished, but the XRD pattern is noisy, and some additional peaks are present. When the reaction was carried out at pH 10, the obtained XRD pattern could not be matched to any known phase.

The morphologies of the samples prepared at 1 mmol of SDS and different pH values were characterized by SEM, as shown in Figure 3 (all presented SEM images are of samples after annealing). One millimole of the surfactant was chosen as the amount used in the reaction based on our previous experience with rare-earth tungstate syntheses in the presence of a surfactant.[19] Preliminary experiments showed that amounts lower than 1 mmol caused the microstructures to be more aggregated. Using higher amounts usually did not show any differences. Occasionally, some cracks were visible on the surface of the microstructures. As can be seen in Figure 3a–c, when the synthesis was carried out at pH 3, spherical microstructures built from nanosized building blocks were obtained as the product. The microstructures had a quite broad size distribution; usually, the diameter of these microspheres was between 2 and 5 μm. It can be observed that the nanobuilding blocks were regular and very tightly packed together. When the pH of the reaction was raised to 7, microspheres again formed (Figure 3d–f). These microstructures had an average diameter between 1 and 3 μm and were built from irregularly shaped nanobuilding blocks. These building blocks were varied in their size and shape and were tightly packed to form the spherical structures. When the pH of the reaction was 10, microspheres several micrometers in size formed (Figure 3g,h). They were built from regular rods stacked together to form the microspheres. Although these architectures were quite regular in their size, occasionally, some of the microspheres had larger rods growing from the cores of these structures. Based on the observed XRD patterns and SEM images, the microstructures synthesized at pH 3 were chosen

dx.doi.org/10.1021/ic5005837 | Inorg. Chem. 2014, 53, 9498−9508

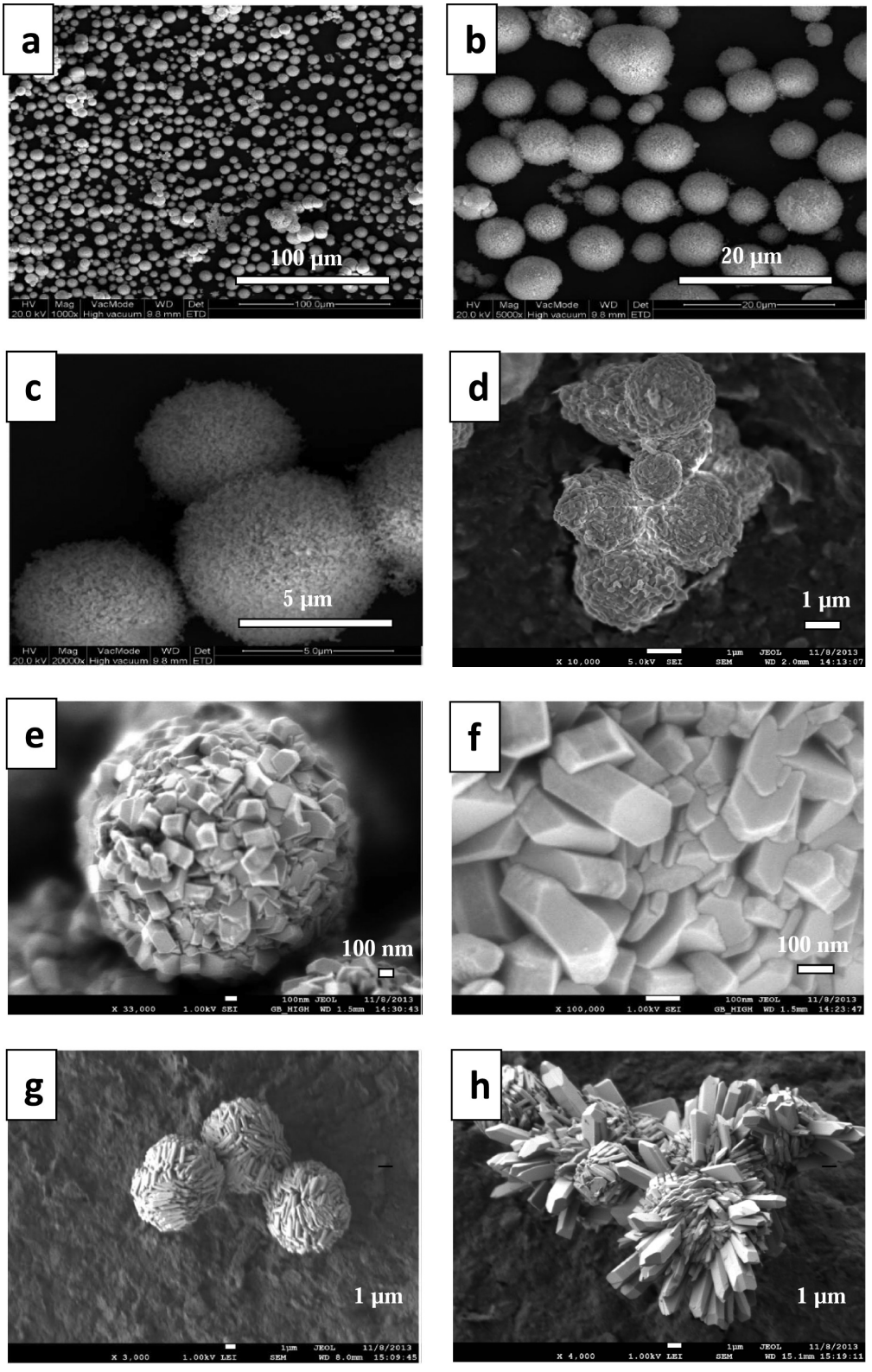

Figure 3. SEM images of annealed samples synthesized at different pH values: (a–c) pH 3, (d–f) pH 7, (g–h) pH 10.

for further studies on the photoluminescence properties of Ln^{3+}-doped Y_2WO_6.

3.2. Luminescence Properties. Rare-earth tungstates have been reported to be good host lattices for the luminescence of lanthanide ions.[22−24] Yttrium compounds are suitable hosts, because their 4f shells are empty and, therefore, no f–f transitions are possible unless other lanthanide ions are incorporated into the materials. As is well-known, tungstate materials emit blue-green light themselves under ultraviolet excitation.[5] The excited tungstate groups can effectively transfer energy to doped lanthanide ions. In this study, we investigated the photoluminescence properties of Sm^{3+}-, Eu^{3+}-, and Dy^{3+}-

dx.doi.org/10.1021/ic5005837 | Inorg. Chem. 2014, 53, 9498−9508

doped Y_2WO_6 samples prepared from nitrate salts, in the presence of 1 mmol SDS, at pH 3, before and after annealing at 1100 °C. Lanthanide-ion concentrations of 2.5%, 5%, and 10% were doped into the Y_2WO_6 matrix. For the optimal lanthanide-ion concentrations, the systems were codoped with 2% or 10% Gd^{3+} ions to test the possible enhancement of luminescence through energy transfer from W−O and/or Gd^{3+} to Ln^{3+}.

3.2.1. Luminescence of Sm^{3+}-, Eu^{3+}-, and Dy^{3+}-Doped Y_2WO_6 Samples. Figures 4−6 present room-temperature

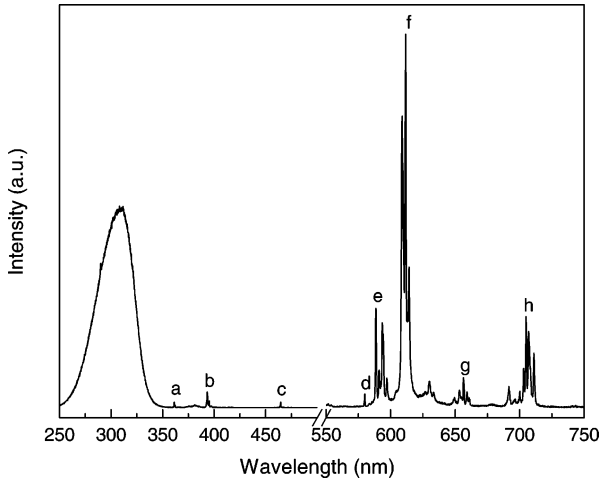

Figure 4. Excitation spectrum (monitored at 611.6 nm) and emission spectrum (excited at 302.0 nm) of a 2.5% Eu:Y_2WO_6 sample. The electronic transitions labeled a−h are assigned in Table 1.

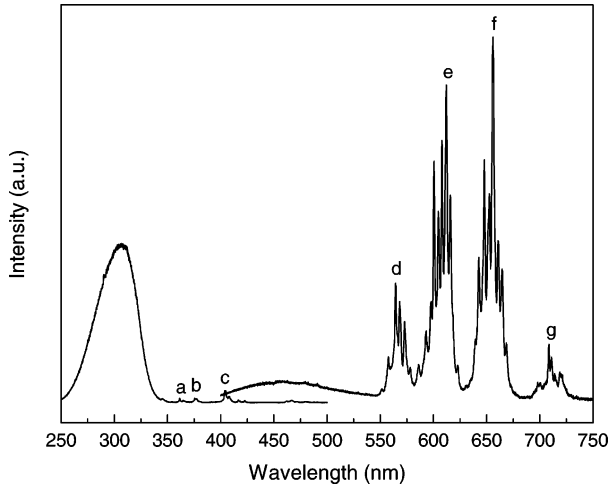

Figure 5. Excitation spectrum (monitored at 655.9 nm) and emission spectrum (excited at 302.0 nm) of a 2.5% Sm:Y_2WO_6 sample. The electronic transitions labeled a−g are assigned in Table 1.

combined excitation−emission spectra of 2.5% Ln^{3+}-doped Y_2WO_6 (Ln = Sm^{3+}, Eu^{3+}, Dy^{3+}) samples after annealing at 1100 °C. The assignments of the observed electronic transitions can be found in Table 1. The excitation spectra all contain a strong and broad band at 250−350 nm and a series of sharp excitation peaks (low in intensity compared to the broad band) that can be assigned to typical intra-4f transitions of lanthanide ions.[25,26] The broad band corresponds to the charge-transfer absorption from the 2p orbitals of the oxygens to the 5d orbitals of tungsten. The emission spectra were obtained upon excitation into the O−W charge-transfer band at

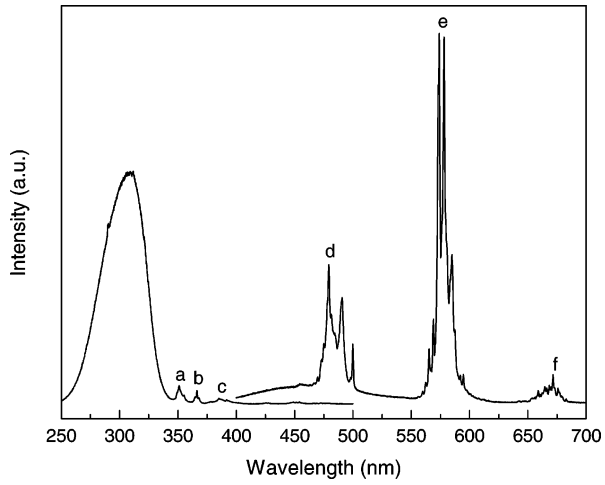

Figure 6. Excitation spectrum (monitored at 574.0 nm) and emission spectrum (excited at 302.0 nm) of a 2.5% Dy:Y_2WO_6 sample. The electronic transitions labeled a−f are assigned in Table 1.

302.0 nm. The emission spectra contain sharp emission peaks characteristic of Eu^{3+}, Sm^{3+}, and Dy^{3+} ions. In the cases of Sm^{3+} and Dy^{3+}, weak broad O−W bands can also be observed in the emission spectra (the Eu:Y_2WO_6 emission spectrum is presented from 550 nm, as there was no broad band in the range of 400−550 nm). The fact that these charge-transfer bands are so weak or not present at all indicates that there is an efficient transfer of energy from the tungstate groups to the doped lanthanide ions. In the emission spectrum of the 2.5% Eu:Y_2WO_6 sample, the $^5D_0 \rightarrow {}^7F_1$ transition peak (Figure 4, peak e) splits into more than three peaks, indicating that more than one Y^{3+} crystallographic site is occupied by Eu^{3+} ions.[27]

The luminescence decay curves of 2.5% Eu-, Sm-, and Dy-doped Y_2WO_6 were measured when excited at 302.0 nm and monitored at the appropriate wavelength. The decay curves could be well-fitted using the single-exponential expression

$$I = I_0 \exp\left(-\frac{t}{\tau}\right) \quad (1)$$

where I and I_0 are the luminescence intensities at times t and 0, respectively, and τ is the luminescence lifetime. The luminescence lifetime of 10% Eu:Y_2WO_6 was found to be 652 μs. For 2.5% Sm:Y_2WO_6 and 2.5% Dy:Y_2WO_6, the lifetimes were calculated to be 272 and 112 μs, respectively. Absolute quantum yields of these samples were determined using an integrating sphere. Quantum yield (QY) is a measure of the ratio of the number of photons emitted by a sample to the number of photons absorbed. Quantum yield can be calculated using the equation

$$\eta = \frac{L_{\text{emission}}}{E_{\text{blank}} - E_{\text{sample}}} \quad (2)$$

where L_{emission} is the integrated area under the emission spectrum, E_{blank} is the integrated area under the "excitation" band of the blank, and E_{sample} is the integrated area under the excitation band of the sample (as the sample absorbs part of the light, this area will be smaller than E_{blank}). The QY of 2.5% Eu:Y_2WO_6 was calculated to be 53%. QYs for 2.5% Sm:Y_2WO_6 and 2.5% Dy:Y_2WO_6 were found to be 8% and 17%, respectively.

dx.doi.org/10.1021/ic5005837 | Inorg. Chem. 2014, 53, 9498−9508

Table 1. Assignment of Labeled Transitions Shown in Figures 4−6

	excitation				emission			
	wavelength (nm)	energy (cm^{-1})	transition		wavelength (nm)	energy (cm^{-1})	transition	
			2.5% $Eu:Y_2WO_6$					
a	361.2	27686	$^5D_4$	← $^7F_0$	d	579.9	17244	$^5D_0$ → $^7F_0$
b	393.3	25426	$^5L_6$		e	588.6	16989	$^7F_1$
c	464.6	21524	$^5D_2$		f	611.8	16345	$^7F_2$
					g	656.5	15232	$^7F_3$
					h	705.0	14184	$^7F_4$
			2.5% $Sm:Y_2WO_6$					
a	361.6	27655	$^4D_{5/2}$, $^6P_{5/2}$, $^4D_{3/2}$	← $^6H_{5/2}$	d	564.4	17718	$^4G_{5/2}$ → $^6H_{5/2}$
b	376.3	26574	$^6P_{7/2}$		e	612.1	16337	$^6H_{7/2}$
c	403.7	24771	$^6P_{3/2}$		f	656.2	15239	$^6H_{9/2}$
					g	708.4	14116	$^6H_{11/2}$
			2.5% $Dy:Y_2WO_6$					
a	350.9	28498	$^6P_{7/2}$	← $^6H_{15/2}$	d	479.3	20864	$^4F_{9/2}$ → $^6H_{15/2}$
b	366.2	27308	$^6P_{5/2}$, $^4P_{3/2}$, $^4D_{3/2}$, $^4M_{19/2}$		e	574.0	17422	$^6H_{13/2}$
c	385.2	25961	$^4I_{13/2}$, $^4F_{7/2}$		f	671.6	14890	$^6H_{11/2}$

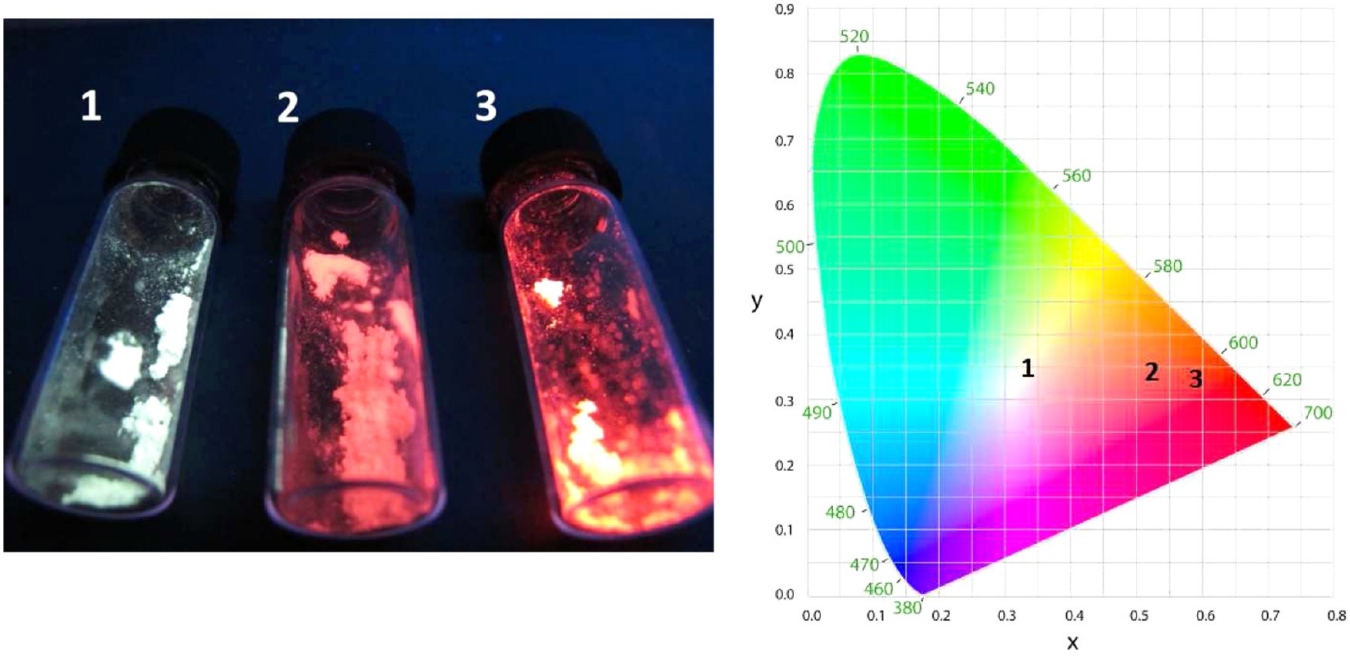

Figure 7. Photograph and CIE color coordinate diagram of Y_2WO_6 doped with 2.5% (1) Dy^{3+}, (2) Sm^{3+}, and (3) Eu^{3+}. The photograph was taken when the samples were excited at 302 nm with a laboratory UV lamp.

It was observed that, under a laboratory UV lamp (302 nm excitation), the 2.5% Eu-, Sm-, and Dy-doped samples showed red, orange-pink, and white colors, respectively (Figure 7). Figure 7 also presents the CIE chromaticity diagram of these samples based on the emission spectral data and color-matching functions issued by CIE in 1931. The CIE coordinates for 2.5% $Eu:Y_2WO_6$ were determined to be $x = 0.581$, $y = 0.338$. The CIE coordinates for 2.5% $Sm:Y_2WO_6$ were determined to be $x = 0.510$, $y = 0.344$. For the 2.5% $Dy:Y_2WO_6$ sample, the CIE coordinates were calculated to be $x = 0.324$, $y = 0.353$. These coordinates are close to those of standard white light ($x = 0.333$, $y = 0.333$).

The color temperature of the white-emitting 2.5% $Dy:Y_2WO_6$ sample was determined to be 4428 K. The color temperature is a measurement in Kelvin that indicates the tone of a specific type of light source. The 2.5% $Dy:Y_2WO_6$ sample falls under the category of neutral white light. Neutral white-light sources reveal a clear, white light with little blue or red tones. This is the type of light most often used in office areas.

The influence of the doped-ion concentration on the photoluminescence properties of these materials was investigated. In addition to the 2.5% doped samples, materials with 5% and 10% of the doping ion were also synthesized. It was observed that, for the $Eu:Y_2WO_6$ material with the increase in Eu^{3+} ion concentration, the emission intensity, decay time, and QY increased (when the Eu^{3+} doping concentration was increased above 10%, the emission intensity, decay time, and QY started to drop). The emission spectra of $Eu:Y_2WO_6$ samples with different doping concentrations are compared in Figure 8. The decay times and QYs are collected in Table 2. Figure 9 shows the decay curves of $Eu:Y_2WO_6$ samples with different doping concentrations. As can be seen, the 10% Eu-

dx.doi.org/10.1021/ic5005837 | Inorg. Chem. 2014, 53, 9498−9508

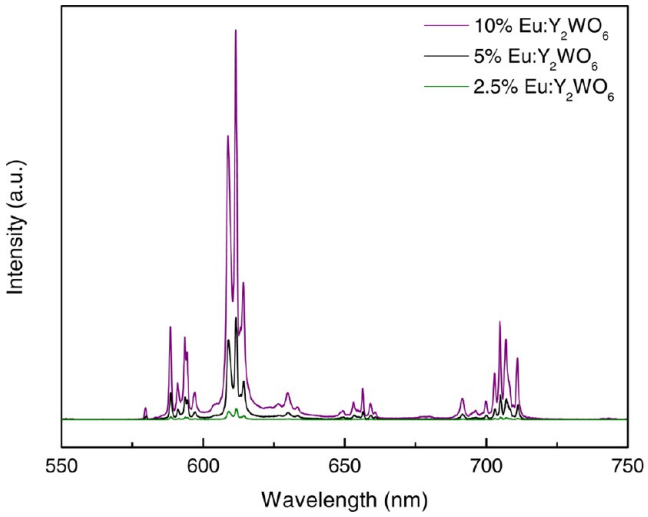

Figure 8. Emission spectra of Eu^{3+}- (2.5%, 5%, and 10%) doped Y_2WO_6 microstructures excited at 302.0 nm (analogous spectra of Sm^{3+}- and Dy^{3+}-doped Y_2WO_6 can be found in the Supporting Information, Figures S6 and S7, respectively).

Table 2. Decay Times and QY Values of the Studied Y_2WO_6 Doped Samples

sample	decay (μs)	quantum yield (%)
2.5% Eu:Y_2WO_6	559	53
5% Eu:Y_2WO_6	588	56
10% Eu:Y_2WO_6	652	68
2.5% Eu_2% Gd:Y_2WO_6	651	62
2.5% Eu_10% Gd:Y_2WO_6	582	37
10% Eu_2% Gd:Y_2WO_6	701	79
10% Eu_10% Gd:Y_2WO_6	566	33
2.5% Sm:Y_2WO_6	272	8
5% Sm:Y_2WO_6	180	3
10% Sm:Y_2WO_6	114	1
2.5% Sm_2% Gd:Y_2WO_6	320	11
2.5% Sm_10% Gd:Y_2WO_6	420	19
2.5% Dy:Y_2WO_6	119	17
5% Dy:Y_2WO_6	78	4
10% Dy:Y_2WO_6	56	2
2.5% Dy_2% Gd:Y_2WO_6	155	21
2.5% Dy_10% Gd:Y_2WO_6	160	22

doped sample had the longest decay time. Also, the 10% Eu:Y_2WO_6 material showed a QY as high as 68%. Unlike for the Eu^{3+}-doped materials, the Sm:Y_2WO_6 and Dy:Y_2WO_6 samples showed a different tendency. The 2.5% doped samples were found to have the strongest luminescence emissions, longest decay times, and highest QY values. With the rise in dopant concentration, these values gradually decreased. The exact decay times and QYs can also be found in Table 2. For some of the samples, there was a slight change in the emitted colors with the change in dopant-ion concentration. As mentioned previously, the 2.5% Dy:Y_2WO_6 material emitted white light under 302 nm excitation. The 5% and 10% Dy^{3+}-doped samples showed white-yellow light instead of pure white light. The color temperatures for the 5% and 10% Dy^{3+}-doped samples were calculated to be 4428 and 3880 K, respectively.

It is expected that, with an increase in the Ln^{3+}-ion concentration, the decay time should decrease as a result of concentration quenching. As can be seen from the results

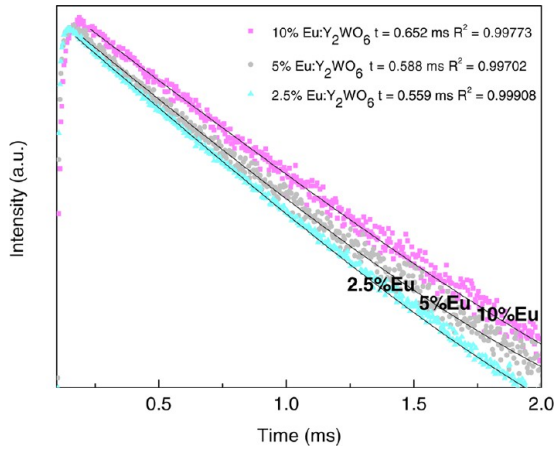

Figure 9. Luminescence decay curves for Eu:Y_2WO_6 (2.5%, 5%, and 10%) with λ_{ex} = 302.0 nm and λ_{em} = 611.6 nm. Black solid lines represent the fitting results.

discussed above, the optimal concentration of Eu^{3+} in the Y_2WO_6 material was found to be 10%, whereas for Sm^{3+} and Dy^{3+}, the optimal concentration was 2.5%. After Y_2WO_6 was doped with Eu^{3+} concentrations above 10%, a decrease in these values was also observed. The low critical quenching concentration of the Sm^{3+} and Dy^{3+} ions (compared to Eu^{3+} ions) might be due to the cross-relaxation effect of these ions. For dysprosium, this process can be written as Dy^{3+} ($^4F_{9/2}$) + Dy^{3+} ($^6H_{15/2}$) → Dy^{3+} ($^6F_{3/2}$) + Dy^{3+} ($^6F_{11/2}$), and for samarium, it is given by Sm^{3+} ($^4G_{5/2}$) + Sm^{3+} ($^6H_{5/2}$) → 2 Sm^{3+} ($^6F_{9/2}$). Eu^{3+} ions have a higher quenching concentration, as no such cross-relaxation effect exists for these ions (in general, the cross-relaxation effect will cause the activator ion to have a low quenching concentration).

Additionally, the luminescence properties of the precursor materials (as-synthesized materials without annealing at 1100 °C) were investigated and compared with the Y_2WO_6 materials. In all cases, the excitation spectra of the precursor samples were similar to those of the heat-treated ones, yet a shift of the broad O−W charge-transfer band toward lower wavelengths was observed in the precursor samples (see Figure S8, Supporting Information). Also, from the relative intensities of the f−f transitions compared to the broad charge-transfer band, it can be estimated that the energy transfer was less efficient than in the heat-treated systems. This might be due to the conversion from distorted tungstate groups in the precursor material to regular tungstate groups in the heat-treated material.[20] Differences can be observed in the emission spectra. In the precursor samples of 2.5% Sm:Y_2WO_6 and 2.5% Dy:Y_2WO_6, the characteristic f−f transition peaks of these lanthanides are partially overlapped with strong, broad charge-transfer bands (Figure 10). The presence of these bands indicates that the transfer of energy from the tungstate groups to the lanthanide ions is not as efficient as in the heat-treated samples. Because of this strong broad band, there is a significant difference in the color that the Sm^{3+}-doped precursor samples emit compared to the heat-treated samples. The 2.5%, 5%, and 10% Sm:Y_2WO_6 precursor samples all gave white light when excited with a 302 nm laboratory lamp. After heat treatment, in all cases, the emission color changed to orange-pink. The Dy^{3+}-doped precursor samples also showed white-light emission at the three investigated ion concentrations (according to the CIE color diagram, the samples gave a bluish-white light, although

dx.doi.org/10.1021/ic5005837 | Inorg. Chem. 2014, 53, 9498−9508

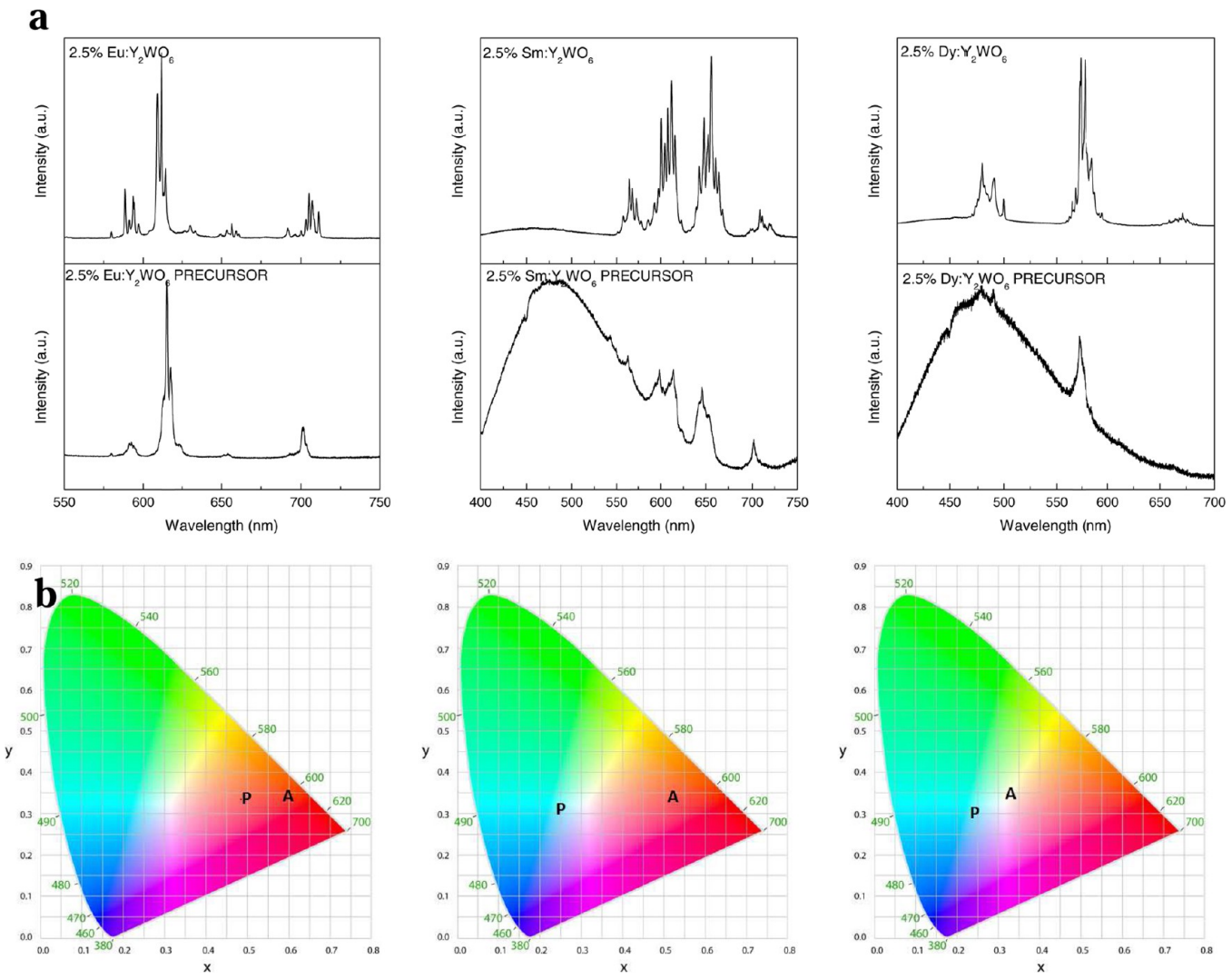

Figure 10. (a) Comparison of the emission spectra of 2.5% Eu-, Sm-, and Dy-doped Y_2WO_6 samples (bottom) before and (top) after heat treatment at 1100 °C. The precursor samples were excited at 283.0 nm, whereas the heat-treated samples were excited at 302.0 nm. (b) CIE coordinates shown on color diagrams: (P) precursor and (A) annealed samples.

the blue component was not visible when the samples were excited with a UV lamp). In all of the Ln^{3+}-doped precursor materials, the decay times were significantly shorter, and the QYs were notably lower compared to those of the annealed materials (Table S1, Supporting Information).

3.2.2. Luminescence of Gd^{3+}-Codoped Y_2WO_6 Samples. It is known that Gd^{3+}, as well as Bi^{3+}, Li^+, K^+, and other ions, can be codoped into phosphor materials to improve their luminescence properties.[28−32] To the best of our knowledge, a Gd^{3+}-codoped system has not yet been reported for any materials belonging to the rare-earth tungstate family. Unlike in the case of codoping of a material with Bi^{3+} ions, which leads to a shift of the excitation band to longer wavelengths, incorporating Gd^{3+} ions into the matrix does not cause any changes in the excitation spectra (Figure S9, Supporting Information). The reasoning for the improvement of luminescence properties of a Ln^{3+}-doped material after codoping with Gd^{3+} ions is still not quite understood, and different energy-transfer mechanisms have been proposed by researchers.[28,30,33−37] It is likely that the presence of the Gd^{3+} ions in the material increases the luminescence properties of Eu^{3+}-, Sm^{3+}-, and Dy^{3+}-doped Y_2WO_6 because Gd^{3+} ions have better matching energy levels to accept the energy from the tungstate matrix and subsequently pass it on to the Eu^{3+}, Sm^{3+}, and Dy^{3+} ions. Also, the increase of the luminescence properties (emission intensity, luminescence lifetime, and quantum yield) could be due to the change of local crystal field of the Ln^{3+} ions after the codoping of Gd^{3+} ions into the matrix.

Gd^{3+} ions at concentrations of 2% and 10% were codoped into the Y_2WO_6 materials with the optimal Ln^{3+} concentrations (Ln = Eu^{3+}, Sm^{3+}, Dy^{3+}). The excitation peaks of Gd^{3+} assigned to its intra-4f transitions are usually reported in the 250−300-nm region.[38] These peaks were not visible in the excitation spectra of the Gd^{3+}-codoped Ln^{3+}:Y_2WO_6 samples, as this region is overlapped with the broad and intensive O−W charge-transfer band. The emission peak of Gd^{3+} was also not visible in the emission spectra of these samples.

It was observed that the incorporation of Gd^{3+} ions into the Ln^{3+}-doped Y_2WO_6 matrix did not have an effect on the peak splitting and relative peak intensities in excitation or emission spectra, but changed the photoluminescence intensity significantly. For the Eu:Y_2WO_6 material, the 10% Eu^{3+}-doped sample was chosen to test the effect of codoping with Gd^{3+} ions, because the 10% Eu^{3+} doping in this material showed the best

dx.doi.org/10.1021/ic5005837 | Inorg. Chem. 2014, 53, 9498−9508

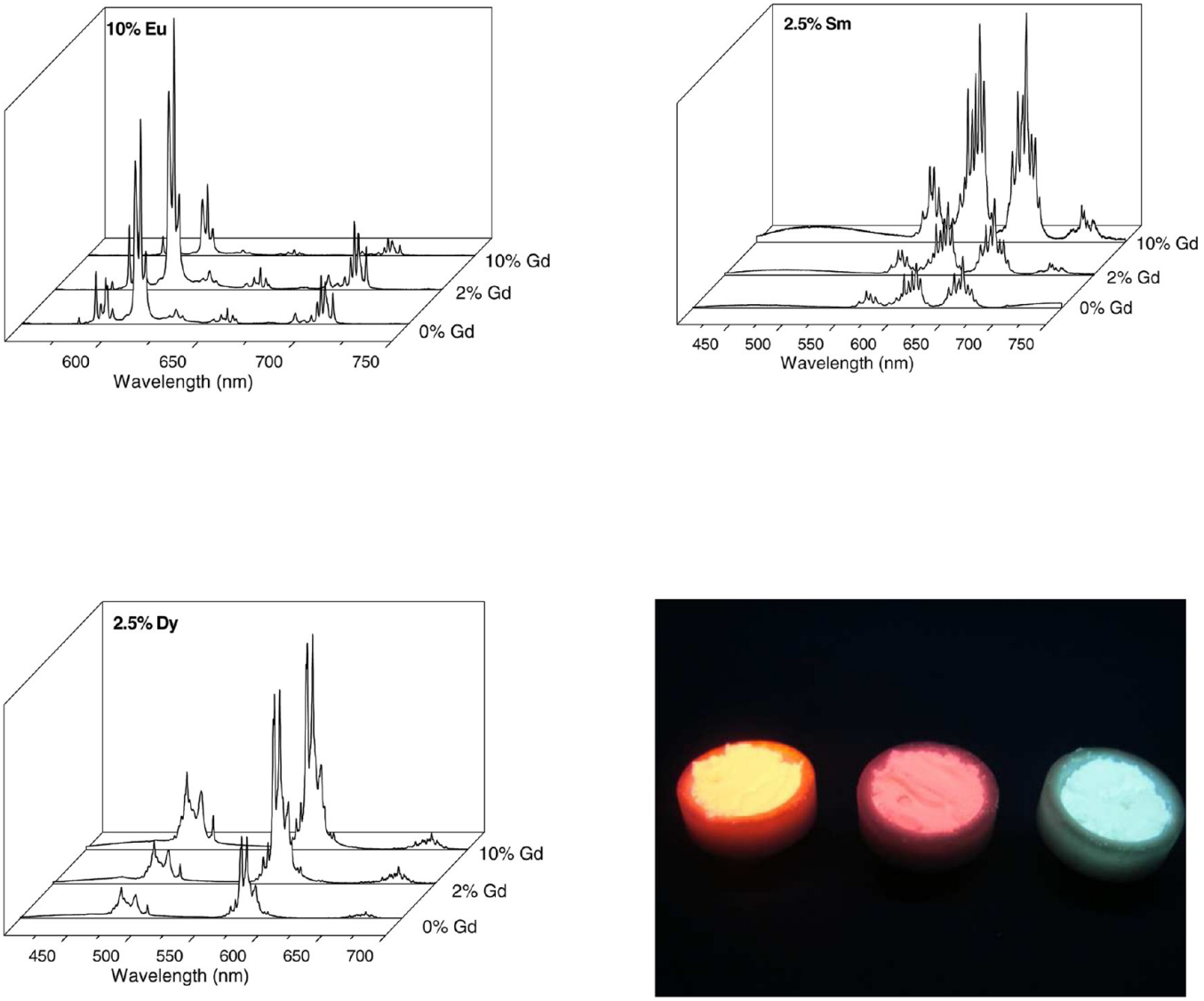

Figure 11. Changes in emission intensity observed for 10% Eu:Y_2WO_6, 2.5% Sm:Y_2WO_6, and 2.5% Dy:Y_2WO_6 codoped with 0%, 2%, and 10% Gd^{3+} ions. The photograph presents the most efficient doped Y_2WO_6 systems as seen under a 302 nm UV lamp (from left to right): 10% Eu_2% Gd:Y_2WO_6, 2.5% Sm_10% Gd:Y_2WO_6, and 2.5% Dy_10% Gd:Y_2WO_6. The colors seen under the UV lamp are slightly different than those suggested by the calculated CIE coordinates.

results (see Figure 11 and Table 2). The QY of 10% Eu_2% Gd:Y_2WO_6 was calculated to be 79%. Therefore, there was an increase in QY compared to that of the 10% Eu:Y_2WO_6 system (QY = 68%). When the amount of codoped Gd^{3+} ions was increased to 10%, a drop in emission intensity, as well as decay time and QY value, was observed. The QY dropped to 33% in this system (see Figure 11 and Table 2). This can most likely be explained by quenching effects when the codoping percentage of Gd^{3+} ions was so high.[30] Concentration quenching is a manifestation of the Förster nonradiative energy-transfer phenomenon.[38,39] It is characterized by a decrease in the QY value as the concentration of the dopant is increased. This phenomenon is most likely caused by the increase in the number of nonradiative decay channels. Additionally, the 2.5% Eu:Y_2WO_6 material was also codoped with 2% and 10% Gd^{3+} ions. In the case when 2% Gd^{3+} was incorporated into the matrix, an increase in luminescence intensity, decay time, and QY was observed (QY = 62%). Codoping the system with 10% Gd^{3+} again caused these values to decrease (QY = 37%). From these experiments, it can be concluded that, for Eu:Y_2WO_6, the 10% Eu_2% Gd:Y_2WO_6 system was the most efficient. The 2.5% doped Sm^{3+} and Dy^{3+} materials were also codoped with Gd^{3+} ions. They were chosen for this experiment because the 2.5% doped Sm^{3+} and Dy^{3+} materials showed the longest decay times and highest QYs. In both cases, with the incorporation of both 2% and 10% Gd^{3+} ions, the luminescence efficiency increased. The highest QY values were measured for the 2.5% Sm_10% Gd:Y_2WO_6 and 2.5% Dy_10% Gd:Y_2WO_6 samples: 19% and 22%, respectively. This means that the QY of the 2.5% Sm material with 10% Gd^{3+} is approximately 2.4 times larger than that of the 2.5% Sm material. For the 2.5% Dy doped material, the increase was not that significant. Some slight changes in the emitted colors were also detected. This was especially noticeable for the Dy^{3+} system, where, after codoping with Gd^{3+}, the sample emitted pale yellow (although a shade of blue was seen when the sample was observed under a 302 nm UV lamp) instead of white light (see Figure 11). The color temperature of the 2.5% Dy_10% Gd:Y_2WO_6 sample was

dx.doi.org/10.1021/ic5005837 | Inorg. Chem. 2014, 53, 9498−9508

determined to be 3591 K (compared to 4428 K for the sample with no codoped Gd^{3+} ions). Therefore, codoping the 2.5% Dy:Y_2WO_6 sample with 10% Gd^{3+} ions shifted the color toward warm white (halogen white). Table 2 summarizes the decay times and QY values of all of the discussed materials. Values for as-prepared samples (precursor samples) can be found in the Supporting Information (Table S1). Table 3 presents the calculated CIE coordinates and colors assigned to these coordinates for all of the materials discussed in this work.

Table 3. Comparison of CIE Chromaticity Coordinates for Ln^{3+}-Doped Y_2WO_6 Samples and Ln^{3+}-Doped Y_2WO_6 Precursor Samples

material	CIE x	CIE y	color
	Eu^{3+}		
2.5% Eu:Y_2WO_6 precursor	0.484	0.334	orange-pink
2.5% Eu:Y_2WO_6	0.581	0.338	red
2.5% Eu_2% Gd:Y_2WO_6	0.590	0.333	red
2.5% Eu_10% Gd:Y_2WO_6	0.646	0.354	reddish orange
5% Eu:Y_2WO_6 precursor	0.568	0.336	red
5% Eu:Y_2WO_6	0.636	0.344	reddish orange
10% Eu:Y_2WO_6 precursor	0.629	0.335	reddish orange
10% Eu:Y_2WO_6	0.643	0.346	reddish orange
10% Eu_2% Gd:Y_2WO_6	0.641	0.347	reddish orange
10% Eu_10% Gd:Y_2WO_6	0.639	0.343	reddish orange
	Sm^{3+}		
2.5% Sm:Y_2WO_6 precursor	0.240	0.304	white
2.5% Sm:Y_2WO_6	0.510	0.344	orange-pink
5% Sm:Y_2WO_6 precursor	0.245	0.308	white
5% Sm:Y_2WO_6	0.523	0.349	orange-pink
10% Sm:Y_2WO_6 precursor	0.266	0.317	white
10% Sm:Y_2WO_6	0.537	0.354	orange-pink
2.5% Sm_2% Gd:Y_2WO_6	0.525	0.344	orange-pink
2.5% Sm_10% Gd:Y_2WO_6	0.442	0.329	orange-pink
	Dy^{3+}		
2.5% Dy:Y_2WO_6 precursor	0.238	0.306	white
2.5% Dy:Y_2WO_6	0.324	0.353	white
5% Dy:Y_2WO_6 precursor	0.241	0.310	white
5% Dy:Y_2WO_6	0.372	0.392	white
10% Dy:Y_2WO_6 precursor	0.245	0.307	white
10% Dy:Y_2WO_6	0.387	0.389	white
2.5% Dy_2% Gd:Y_2WO_6	0.408	0.415	white
2.5% Dy_10% Gd:Y_2WO_6	0.372	0.390	white

3. CONCLUSIONS

In this article, we have presented the synthesis of Eu^{3+}-, Sm^{3+}-, and Dy^{3+}-doped Y_2WO_6 materials, in the presence of SDS surfactant, using a simple hydrothermal method. SDS was used as a directing agent for the synthesis of the rare-earth tungstate materials. By changing the pH value of the starting solution, different phases and phase purities were obtained. At pH 3, the synthesis gave a pure monoclinic Y_2WO_6 phase. It was shown that, by varying the dopant-ion concentration and by codoping the Y_2WO_6 materials with different concentrations of Gd^{3+} ions, the emission intensities, decay times, quantum yields, and colors emitted by the samples could be easily tuned. Some of the obtained samples were single-material sources of white light. For example, the 2.5% Dy:Y_2WO_6 sample emitted white light when excited at 302.0 nm. The QY of this white-emitting material was evaluated to be 17%. The most efficient system was observed for 10% Eu_2% Gd:Y_2WO_6, for which the QY reached 79%. Incorporating 10% Gd^{3+} ions into the 2.5% Sm:Y_2WO_6 material gave a QY approximately 2.4 times larger than that of the material with no Gd^{3+} ions. Among the studied systems, the Sm^{3+},Gd^{3+}-codoped system showed the highest increase in efficiency compared to the system without codoped Gd^{3+} ions.

■ ASSOCIATED CONTENT

Supporting Information

Standard XRD pattern of monoclinic Y_2WO_6 calculated using the Mercury crystal structure visualization, exploration, and analysis tool; decay curves of all Eu-, Sm-, and Dy-doped and Gd-codoped Y_2WO_6 samples after annealing at 1100 °C with fits; table with decay times and QY values of Eu-, Sm-, and Dy-doped Y_2WO_6 sample precursors (different ion concentrations); excitation spectra of 2% Gd-codoped samples; emission spectra of Sm- and Dy-doped samples at different dopant concentrations; one excitation spectrum corrected for detector sensitivity. This material is available free of charge via the Internet at http://pubs.acs.org.

■ AUTHOR INFORMATION

Corresponding Authors

*E-mail: Anna.Kaczmarek@Ugent.be.
*E-mail: Rik.VanDeun@Ugent.be.

Notes

The authors declare no competing financial interest.

■ ACKNOWLEDGMENTS

R.V.D. thanks the Hercules Foundation (Project AUGE/09/024 “Advanced Luminescence Setup”) and Ghent University (Project BOF 01N01010) for funding.

■ REFERENCES

(1) Jüstel, T.; Krupa, J.-C.; Wiechert, D. U. *J. Lumin.* **2001**, *93*, 179−189.
(2) Kaminskii, A. A.; Eichler, H. J.; Ueda, K.; Klassen, N. V.; Redkin, B. S.; Li, L. E.; Findeisen, J.; Jaque, D.; Garcia-Sole, J.; Balda Fernandez, J. R. *Appl. Opt.* **1999**, *38*, 4533−4547.
(3) Lei, F.; Yan, B. J. *Solid State Chem.* **2008**, *181*, 855−862.
(4) Bünzli, J. C. G.; Piguet, C. *Chem. Soc. Rev.* **2005**, *34*, 1048−1077.
(5) Blasse, G.; Verhaar, H. C. G.; Lammers, M. J. J.; Wingefeld, G.; Hoppe, R.; De Maayer, P. *J. Lumin.* **1984**, *29*, 497−499.
(6) Kaczmarek, A. M.; Van Deun, R. *Chem. Soc. Rev.* **2013**, *42*, 8835−8848.
(7) Liu, X.; Hou, W.; Yang, X.; Liang, J. *CrystEngComm* **2014**, *16*, 1268−1276.
(8) Zhou, Y.; Yan, B.; He, X.-H. *J. Mater. Chem. C* **2014**, *2*, 848−855.
(9) Abtmeyer, S.; Pązik, R.; Wiglusz, R.; Małecka, M.; Seisenbaeva, G. A.; Kessler, V. G. *Inorg. Chem.* **2014**, *53*, 943−951.
(10) Hou, L.; Cui, S.; Fu, Z.; Wu, Z.; Fu, X.; Jeong, J. H. *Dalton Trans.* **2014**, *43*, 5382−5392.
(11) Colfen, H.; Mann, S. *Angew. Chem., Int. Ed.* **2003**, *42*, 2350−2365.
(12) Qian, L.-W.; Wang, X.; Zheng, H.-G. *Cryst. Growth Des.* **2012**, *12*, 271−280.
(13) Zhou, Y.; Yan, B. *CrystEngComm* **2013**, *15*, 5694−5702.
(14) Borchardt, H. J. *J. Chem. Phys.* **1963**, *39*, 504−511.
(15) Efremov, V. A.; Tyulin, A. V.; Trunov, V. K.; Kudin, O. V.; Yanovskii, V. K.; Voronkova, V. I. *Kristallografiya* **1984**, *29*, 904−909.
(16) Beaury, O.; Faucher, M.; De Sagey, G. T. *Acta Crystallogr. B* **1981**, *37*, 1166−1170.
(17) Tyulin, A. V.; Efremov, V. A.; Trunov, V. K. *Kristallografiya* **1989**, *34*, 885−892.

(18) Jinping, H.; Jun, X.; Hengxin, L.; Hongshan, L.; Xibin, Y.; Yinkang, L. *J. Solid State Chem.* **2011**, *184*, 843−847.
(19) Kaczmarek, A. M.; Liu, Y.-Y.; Van Der Voort, P.; Van Deun, R. *Dalton Trans.* **2013**, *42*, 5471−5479.
(20) Huang, S.; Zhang, X.; Wang, L.; Bai, L.; Xu, J.; Li, C.; Yang, P. *Dalton Trans.* **2012**, *41*, 5634−5642.
(21) Wang, J.; Zhang, Z.-J.; Zhao, J.-T.; Chen, H.-H.; Yang, X.-X.; Tao, Y.; Huang, Y. *J. Mater. Chem.* **2010**, *20*, 10894−10900.
(22) Guo, C.; Wang, S.; Chen, T.; Luan, L.; Xu, Y. *Appl. Phys. A: Mater. Sci. Process.* **2009**, *94*, 365.
(23) Zheng, Y.; Li, Z.; Wang, L.; Xiong, Y. *CrystEngComm* **2012**, *14*, 7043−7048.
(24) Hou, Z.; Cheng, Z.; Li, G.; Wang, W.; Peng, C.; Li, C.; Ma, P.; Yang, D.; Kang, X.; Lin, J. *Nanoscale* **2011**, *3*, 1568−1574.
(25) Carnall, W. T.; Fields, P. R.; Rajnak, K. *J. Chem. Phys.* **1968**, *49*, 4424−4442.
(26) Carnall, W. T.; Fields, P. R.; Rajnak, K. *J. Chem. Phys.* **1968**, *49*, 4450−4455.
(27) Görller-Walrand, C.; Binnemans, K. In *Handbook on the Physics and Chemistry of Rare Earths*; Gschneidner, K. A., Jr., Eyring, L., Eds.; Elsevier Science: Amsterdam, 1998; Vol. *25*, Chapter 167, pp 101−264.
(28) Singh, B. P.; Parchur, A. K.; Ningthoujam, R. S.; Ansari, A. A.; Singh, P.; Rai, S. B. *Dalton Trans.* **2014**, *43*, 4779−4789.
(29) Devi, Ch. V.; Phaomei, G.; Yaiphaba, N.; Rajmuhon Singh, N. *J. Alloys Compd.* **2014**, *583*, 259−266.
(30) Ryba-Romanowski, W.; Gołąb, S.; Dominiak-Dzik, G.; Solarz, P. *Appl. Phys. A: Mater. Sci. Process.* **2002**, *74*, 581−586.
(31) Kaur, G.; Dwivedi, Y.; Rai, S. B. *J. Fluoresc.* **2011**, *21*, 423−432.
(32) Xie, M.; Tao, Y.; Liang, H.; Su, Q. *Inorg. Chem.* **2010**, *49*, 11317−11324.
(33) Debasu, M. L.; Ananias, D.; Rocha, J.; Malta, O. L.; Carlos, L. D. *Phys. Chem. Chem. Phys.* **2013**, *5*, 15565−15571.
(34) Li, Y.-C.; Chang, Y.-H.; Chang, Y.-S.; Lin, Y.-J.; Laing, C.-H. *J. Phys. Chem. C* **2007**, *111*, 10682−10688.
(35) Li, Z.; Wang, B.; Xing, L.; Liu, S.; Tan, N.; Xiao, S.; Ding, J. *Chin. Opt. Lett.* **2012**, *10*, 081602−1−081602−4.
(36) Pu, Y.; Tang, K.; Zhu, D.-C.; Han, T.; Zhao, C.; Peng, L.-L. *Nano-Micro Lett.* **2013**, *5*, 117−123.
(37) Pan, Y.; Wu, M.; Su, Q. J. *Phys. Chem. Sol* **2004**, *65*, 845−850.
(38) Carnall, W. T.; Fields, P. R.; Rajnak, K. *J. Chem. Phys.* **1968**, *49*, 4443−4446.
(39) Förster, T. *Discuss. Faraday Soc.* **1959**, *27*, 7−17.
(40) Van Haecke, J. E.; Smet, P. F.; Poelman, D. J. *Electrochem. Soc.* **2005**, *152*, H225−H228.

dx.doi.org/10.1021/ic5005837 | *Inorg. Chem.* 2014, 53, 9498−9508